Retrieval of aerosol parameters using IRS P4 OCM data over the Arabian Sea and the Bay of Bengal

Sagnik Dey and Ramesh P. Singh*

Department of Civil Engineering, Indian Institute of Technology, Kanpur 208 016, India

The recent first-field phase of Indian Ocean Experiment has provided various types of aerosol data over the Arabian Sea, the Bay of Bengal and the Indian Ocean. Using optical sensors on-board numerous satellites, global aerosol parameters have been estimated by many workers. In this communication, we have used IRS P4 OCM data to retrieve the aerosol parameters over the Arabian Sea and the Bay of Bengal. We also discuss the spatial, spectral and temporal variations of aerosol optical depth (AOD) over these regions. The Bay of Bengal shows more dynamic nature of aerosols compared to the Arabian Sea. Aerosol size-distribution shows unimodal nature during winter and bimodal nature during summer season. The spatial gradient of AOD is found to be higher over the Bay of Bengal compared to that over the Arabian Sea. A zone has been found over the Bay of Bengal, which shows low values of AOD (< 0.25) for all the months. The Bay of Bengal experiences much more aerosol loading and transport of aerosols from the Indian subcontinent compared to the Arabian Sea. An aerosol plume is found in the northwestern Arabian Sea during February to March, and it is found to be dispersed in April. The spectral distribution of AOD and the size distribution suggest that the Bay of Bengal is dominated by finer particles compared to the Arabian Sea.

RECENTLY, the remote sensing method has emerged as a powerful technique to study spatial and temporal distributions of aerosols on a global scale. The study of spatial and temporal distributions of aerosols over the ocean is of great importance because of their influence on climate through radiative interactions[1,2]. Aerosols also play a major role in the formation of clouds in the marine boundary layer, which causes changes in the cloud droplet size distribution. As a result changes in the cloud albedo occur, leading to change in radiative coupling between ocean and atmosphere, with climatic implications[3]. Mineral aerosols from continents are found to be transported by winds over to remote oceans and this significantly influences the aerosol characteristics[4]. Attempts have been made to study the aerosol distribution over the tropical ocean during the Indian Ocean Experiment (INDOEX) programme during 1996–2001 (refs 5–8). But it is not possible to monitor the spatial and temporal aerosol distribution from ground regularly, though efforts have been made for the purpose[9]. Ocean colour monitoring sensors IRS P3, IRS P4 OCM and SeaWiFS, primarily designed for ocean colour monitoring, have been proved to be useful in monitoring aerosols over the ocean at frequent intervals[10]. OCM is equipped with the additional band of wavelength greater than 700 nm, where no radiation originates from the water because of high infrared absorption, and all the received radiance is mostly from the atmosphere.

The IRS P4 OCM data used in this communication cover (1) the region bounded by 65.84 to 79.49E longitude and 31.29 to 16.76N latitude, covering part of the Arabian Sea along the western part of India and (2) the region bound by 75.82 to 89.67E longitude and 19.34 to 5.08N latitude, covering southern part of the Bay of Bengal and southeastern part of India. IRS P4 OCM raw data of unsigned 16-bit format[11] have been used for the purpose. The OCM data in eight bands have been imported using ERDAS 8.3.1 and images have been displayed in eight bands. These images are georeferenced by taking suitable ground control points with the help of toposheets of the area. In the present communication, monthly averaged OCM data of January to April 2000 covering the Arabian Sea, and data of November 1999 to May 2000 covering the Bay of Bengal have been used. The land region has been masked.

The radiance detected by a space-borne sensor at the top of the atmosphere (TOA) in the wavelength (λ) can be split into four terms[10]:

$$L_t(\lambda) = L_a(\lambda) + L_r(\lambda) + t_d(\lambda).L_w(\lambda), \quad (1)$$

where L_t is sensor detected radiance; L_a is aerosol path radiance = $F_o.\omega_{0a}.\tau_a.p_a/(4\pi\cos\theta_v)$; L_r is Rayleigh path radiance = $F_o.\omega_{0r}.\tau_r.p_r/(4\pi\cos\theta_v)$; L_w is water-leaving radiance; ω_{0a} is aerosol scattering albedo; ω_{0r} is Rayleigh single scattering albedo; θ_v is satellite viewing zenith angle; τ_a/τ_r is aerosol/Rayleigh optical depth; p_a/p_r is aerosol/Rayleigh scattering phase function; $t_d = \exp[-(1/\cos\theta_v + 1/\cos\theta_s)(\tau_r/2 + \tau_{oz})]$ is atmospheric diffuse transmittance; θ_s is solar zenith angle, and τ_{oz} is ozone absorption optical depth.

In eq. (1), the Rayleigh and aerosol path radiance together constitute the atmospheric path radiance. The phase function is determined using Heyney–Greenstein model[12]. The Rayleigh path radiance is computed as the spectral dependence of the Rayleigh optical depth, and the Rayleigh phase functions are well known. The diffuse transmittance is also calculated from the Rayleigh optical depth and ozone absorption optical depth. The value of the ozone absorption optical depth is taken constant, since its variation within the spectral range of ocean colour sensor is negligible. There will be no water-leaving radiance for wavelengths above 700 nm, due to strong infrared absorption by water. The measured TOA radi-

*For correspondence. (e-mail: ramesh@iitk.ac.in)

ance is just the sum of the aerosol path radiance and Rayleigh path radiance. The aerosol path radiance is calculated from the TOA radiance at 765 and 865 nm wavelengths, knowing the value of Rayleigh radiance at these wavelengths. The aerosol path radiance is computed for the other bands of the OCM, through extrapolation method[12].

The aerosol optical depth is calculated for eight wavelengths from the following equation[10]

$$\tau_a = (L_t - L_r)/[F_o/(p_a.4\pi\cos\theta_v)]. \quad (2)$$

The coastal region, especially the bay region suffers from turbidity and shows higher reflectance values. The retrieval of aerosol optical depth (AOD) from such regions is not found to be accurate and reliable. The algorithm for retrieval of aerosol parameters over turbid water, which is a common feature in bay areas, has been recently used by Okada *et al.*[13]. They have used the ratio of radiance at 412 to 443 nm wavelengths for bay regions, where the concentration of suspended materials is high. The suspended materials absorb highly at 412 nm and less at 443 nm; thus the ratio becomes less. On the other hand, at other places, absorption is less at 412 nm and high at 443 nm wavelengths, and thus the ratio of radiance at 412 to 443 nm becomes large. A value of 1.1 is considered to be the threshold value to distinguish between these two regions. For fixing the threshold, two assumptions have been made: (1) contribution from the atmosphere has large variations, and (2) contribution of water substances with soil particles shows quasi-homogeneous effects at 412 nm. The monthly averaged AOD has been retrieved for coastal and oceanic regions, and the AOD estimation is found to suffer with ± 3% errors.

Figure 1 shows the monthly averaged AOD for eight bands of OCM in the wavelength range 412 to 865 nm

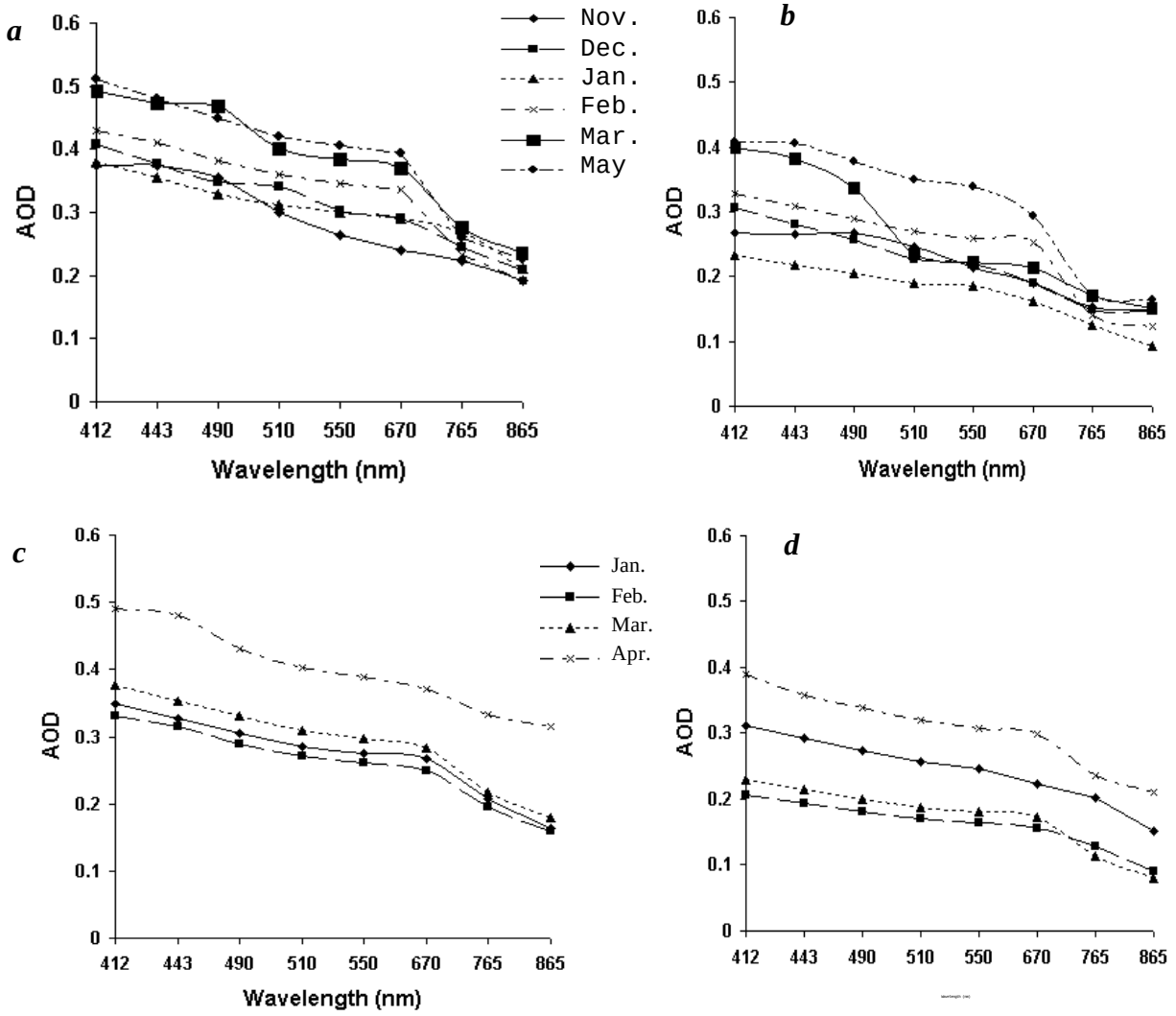

Figure 1. Monthly averaged AOD over (***a***) coastal regions of the Bay of Bengal, (***b***) deeper parts of the Bay of Bengal, (***c***) coastal regions of the Arabian Sea, and (***d***) deeper parts of the Arabian Sea.

over the Arabian Sea and the Bay of Bengal. The large difference in the near-infrared (NIR) and visible AOD is clearly due to the particle size. Over the Bay of Bengal, during the months of November to May, AOD values show two peaks (in the months of December and May; Figure 1). Over the Arabian Sea, AOD value is highest (~ 0.5) in the month of April (Figure 1). AOD sharply increases at wavelength 670 nm compared to that at 765 nm over the Bay of Bengal, whereas over the Arabian Sea, the increase is not so sharp. Higher AOD values have been found over the Bay of Bengal during the summer and winter season compared to those over the Arabian Sea (Figure 1). The difference in AOD has been found to be higher at the shorter wavelength compared to those at longer wavelengths. The large variations in AOD at the longer wavelengths over the Bay of Bengal are due to its dynamic nature and steeper aerosol particle size distribution. This is attributed to the abundance of aerosols and closer proximity to the source regions. The latitudinal variations of AOD over the Bay of Bengal and the Arabian Sea have been obtained by averaging all the AOD values separately for the longitude ranges 64 to 73E (Arabian Sea), and 78 to 90E (Bay of Bengal) during the corresponding months. Figure 2 *a* and *b* shows the latitudinal variations of AOD (at 765 nm) over the Arabian Sea and the Bay of Bengal. During the month of January, AOD is > 0.15 over the Arabian Sea, with the highest value (~ 0.21) close to the west coast of India. In general, AOD over the Arabian Sea is found to be higher in the month of January compared to that in February and March. In April AOD increases further (Figure 2 *a*). An aerosol plume is found to form near the coast of Pakistan over the northwestern Arabian Sea in February. This plume is intensified in March and dispersed in April. This plume has also been found by Rajeev *et al.*[14] during INDOEX field measurements (1998) and using NOAA AVHRR data for the year 1998. The higher values of AOD (0.35–0.4) in the higher latitude (25N) during February and March are due to the generation of this plume. The spatial distribution of AOD over the Bay of Bengal is found to be dynamic. Small variations in the value of AOD for the period from November to May are found in the lower latitude regions of the Bay of Bengal, whereas the variations are large in the higher latitude regions (Figure 2 *b*). AOD values are found to be higher (~ 0.3) in December compared to those in November and January–March. Highest value of AOD has been found during May (~ 0.5 in the coastal regions and ~ 0.3 over the deeper parts of the ocean). An interesting zone has been found in a study by Rajeev *et al.*[14] over the Bay of Bengal (Figure 3), where AOD is low (< 0.25) for all the months. The location of this low-AOD zone is controlled by the interaction[13] of the Inter-Tropical Convergence Zone (ITCZ) with the regional climatic condition. Significant temporal variations have been found over the Bay of Bengal and the Arabian Sea.

Spectral AOD carries information about the particle size. The inverse power law[15] spectral variations of AOD is given as:

$$\tau_p = \beta \lambda^{-\alpha}, \quad (3)$$

where α is the wavelength exponent, β is the turbidity parameter and λ is the wavelength in μm. The value of α depends on the ratio of the concentration of large to small aerosol particles, and β represents the total aerosol loading in the atmosphere[16].

The values of α and β for the Bay of Bengal and the Arabian Sea have been obtained by linear least square fitting of $\tau_p - \lambda$ on a log–log scale[17]. The values of α and β have been obtained over the coastal and the deep ocean regions during winter and summer seasons for the Bay of Bengal and the Arabian Sea (Figure 4 *a* and *b*) using limited data. Values of α and β over the Bay of Bengal for

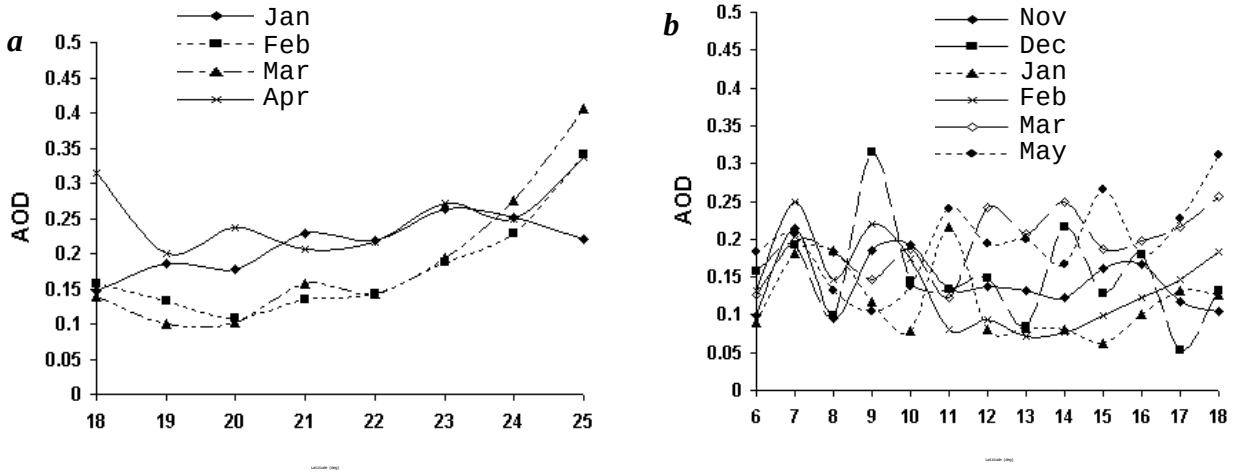

Figure 2. Latitudinal variations of AOD (765 nm) for (***a***) the Arabian Sea sector (65 to 73E) and (***b***) the Bay of Bengal sector (78 to 90E).

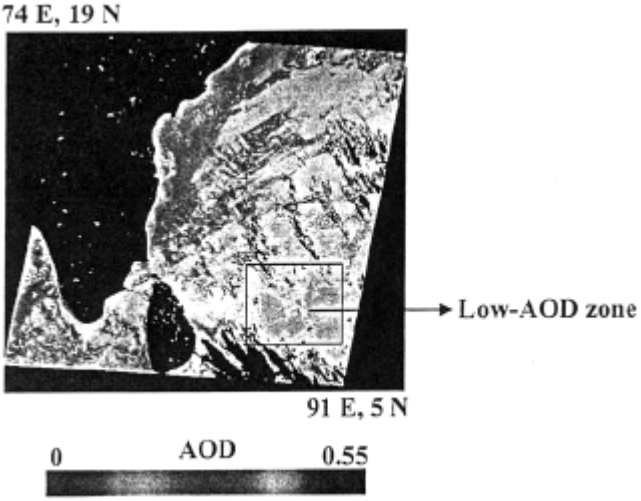

Figure 3. Low-AOD zone (7.3N to 10.7N latitude and 83.6E to 86.9E longitude) over the Bay of Bengal.

winter season have been obtained by averaging the AOD values for the months of November to February, and for summer season by averaging the AOD values for the months of March to May. In case of the Arabian Sea, the values of α and β for winter season have been obtained by averaging the AOD value for the months of January and February, and for summer season by averaging the AOD values for the months of March and April. The value of α in the coastal regions over the Bay of Bengal and the Arabian Sea during winter season has been found to be almost similar (0.9 to 1.1), whereas during the summer season the value is higher (~ 1.4) over the Bay of Bengal compared to that over the Arabian Sea (0.7 to 0.9; Figure 4*a*). Higher value of α indicates the dominance of smaller aerosol particles in the particle size spectrum (0.1 to 5 μm).

During the winter season the subcontinent experiences the northeast monsoon, where the general direction of wind is from northeast to west. This wind carries larger sea-spray aerosol particles from the deeper parts of the Bay of Bengal to the coastal regions, increasing the concentration of larger particles (> 1 μm) over the Bay of Bengal. Over the Arabian Sea, the effect is reverse and the wind carries finer particles (< 1 μm) from the continent to the ocean, thus increasing the concentration of finer particles. This explains the near-equal values of α over the Bay of Bengal and the Arabian Sea during the winter season. During March to May, the Indian subcontinent experiences hot and dry weather and the transport of the aerosols is mainly aided by the intensified sea breeze during this season. Numerous industrial cities lie along the Bay of Bengal coast compared to those along the Arabian Sea coast. As a result, the coastal regions of the Bay of Bengal produce much more continental aerosols compared to those of the Arabian Sea. This gives higher α values in the coastal regions of the Bay of Bengal during summer season. The low α values in the Arabian Sea coastal regions is attributed to the rapid decrease in AOD at the NIR wavelengths compared to those at visible wavelengths (Figure 1*c*). Also, the air mass over the Arabian Sea travels a longer distance and carries larger dust particles due to its proximity to the Indian desert. The spatial gradient of AOD from coast towards deep ocean is found to be higher in the Bay of Bengal (2.7×10^{-4}/km) compared to that in the Arabian Sea (2.61×10^{-4}/km). The value of β is found to be higher over the deep ocean in the Bay of Bengal (0.25) and the Arabian Sea (0.37) during the summer season compared to that (0.237 for the Bay of Bengal and 0.357 for the Arabian Sea) over the coastal regions (Figure 4*b*). This indicates higher aerosol loading over the deeper parts of the ocean during the summer season compared to those over the coastal regions. Almost similar values of β (~ 0.35) during the winter season over the coastal as well as the deep ocean in the Bay of Bengal and the Arabian Sea are attributed to the flat AOD spectrum over the ocean. This also indicates that the concentration of the larger particles does not show significant variations over the deep ocean.

Using aerosol optical depths at eight wavelengths of OCM sensor, the column size distribution function of aerosols has been computed from the following equation[18]:

$$\tau_p(\lambda) = \int \pi r^2 Q_{ext}(r, \lambda, m) n_c(r)\, dr, \quad (4)$$

where r is the particle radius, Q_{ext} is the Mie extinction efficiency parameter, $\tau_p(\lambda)$ is the aerosol optical depth at wavelength λ and n_c is the column size distribution of aerosols. The column size distribution of aerosol is given by Moorthy *et al.*[19]:

$$n_c dr = \int n(r) dr, \quad (5)$$

where $n(r)\, dr$ is the number of particles in unit volume of atmosphere in a size range (dr) centered at r.

Figures 5*a* and *b* show the aerosol size distribution over the coastal and the deep ocean over the Bay of Bengal and the Arabian Sea during the winter and summer season. The particle size distribution during the winter season over the Bay of Bengal and the Arabian Sea has been found to be unimodal, whereas during the summer season the nature of the particle size distribution is bimodal (Figure 5*a* and *b*). This unimodal nature in the particle size distribution explains the similarity in the values of α over the Bay of Bengal and the Arabian Sea. The peak value of the size distribution curve has been found to be higher over the Arabian Sea (0.7 μm) compared to that over the Bay of Bengal (0.5 μm) (Figure 5*a*). It clearly indicates higher concentration of the larger particles over the Arabian Sea compared to those over the Bay of Bengal. The peaks are wider over the coastal

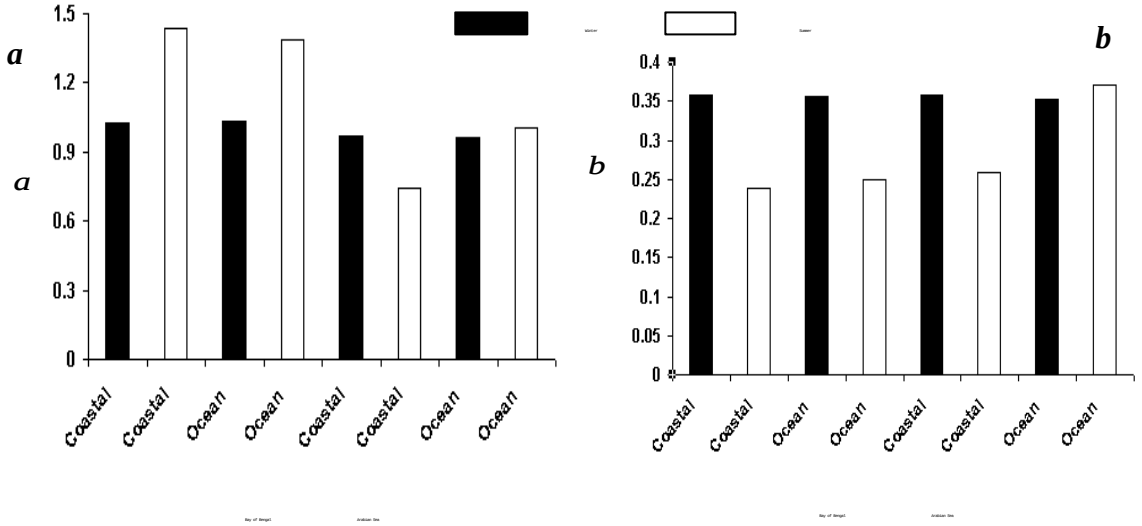

Figure 4. Mean value of (***a***) α and (***b***) β for the Bay of Bengal and the Arabian Sea.

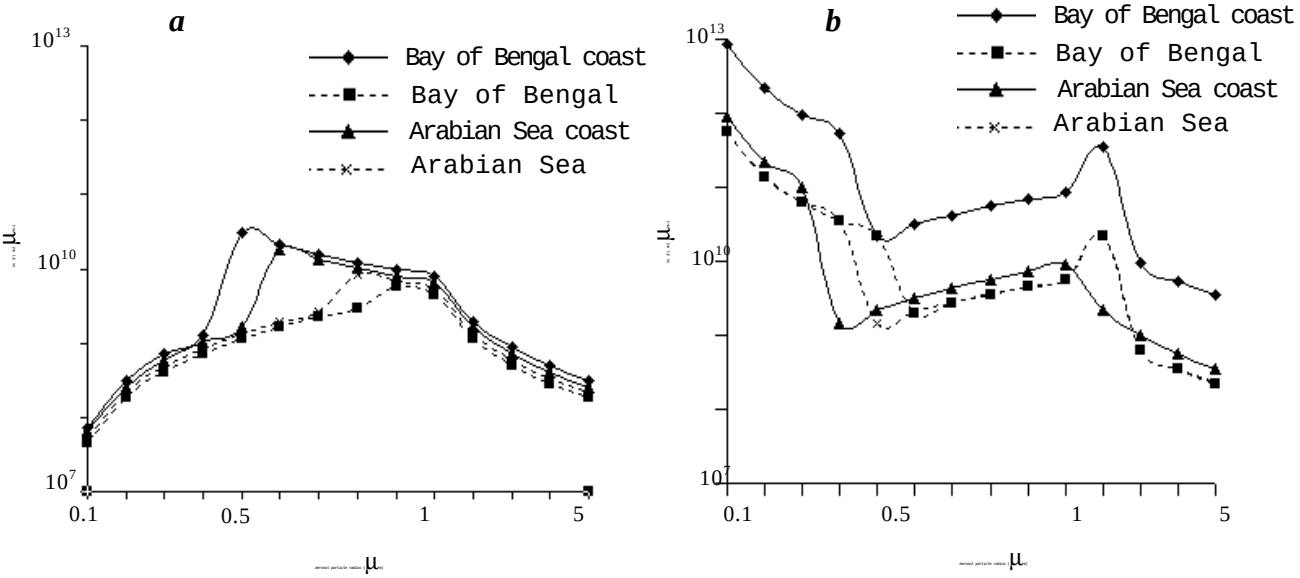

Figure 5. Aerosol size distribution over the Bay of Bengal and the Arabian Sea during (***a***) winter and (***b***) summer.

regions indicating higher concentration of the mixed aerosol particles compared to those over the deeper parts of the ocean. The aerosol particle size distribution over the Bay of Bengal and the Arabian Sea during the summer season has been found to be bimodal in nature (Figure 5*b*), with the second mode at 0.7–1 μm. The higher concentration of the finer particles over the coastal regions of the Arabian Sea during the winter season compared to that of larger particles during the summer season explains the lower value of α (Figure 4*a*). Higher value of the peaks during the summer months, in the aerosol particle size distribution curves (Figure 5*a* and *b*) over the coastal regions of the Bay of Bengal and the Arabian Sea, and the deeper parts of the Bay of Bengal explains explains the higher values of β. Only the deeper parts of the Arabian Sea shows higher aerosol loading during the winter season compared to the summer season[20]. The error bars have been calculated for the aerosol particle size distribution over the Arabian Sea and the Bay of Bengal, and are found to be ± 5%. Since the errors are so small, the error bars are not visible in Figure 5*a* and *b*. The aerosol particle size distribution and the variations of AOD indicate that the Bay of Bengal is much more dynamic compared to the Arabian Sea.

Spectral and temporal distributions of AOD over the Bay of Bengal are found to be much more dynamic compared to those over the Arabian Sea. The spatial gradient of AOD over the Bay of Bengal is found to be higher

compared to that over the Arabian Sea. The greater dominance of finer aerosol particles during the summer season is observed over the coastal regions of the Bay of Bengal compared to those over the Arabian Sea, which indicates greater influence of the continental aerosols over the Bay of Bengal. The particle size distribution during the winter season over the Bay of Bengal and the Arabian Sea is found to be unimodal, whereas during the summer season, it is characterized by bimodal distribution. Higher concentration of the larger particles over the coastal regions of the Arabian Sea during summer is due to the dry conditions prevailing in the western part of the Indian subcontinent and larger transport of dust particles from the continent. An interesting low-AOD zone has been found over the Bay of Bengal.

1. Jaenicke, R., *Aerosols and their Climatic Effects* (eds Gerbard, H. E. and Deepak, A.), Deepak Publishers, USA, 1984, pp. 7–34.
2. Parameswaran, K., *Proc. Indian Natl. Sci. Acad.*, 1998, **64**, 245–266.
3. Charlson, R. J., Lovelock, J. E., Andrea, M. O. and Warren, S. G., *Nature*, 1987, **326**, 655–661.
4. Hoppel, W. A., Fitzgerald, J. W., Frick, G. M. and Larson, R. E., *J. Geophys. Res.*, 1990, **95**, 3659–3686.
5. Rao, Y. Jaya and Devara, P. C. S., *Curr. Sci.*, 2001, **80**, 120–122.
6. Murugavel, P., Pawar, S. D. and Kamra, A. K., *ibid*, 2001, **80**, 123–127.
7. Moorthy, K. K., Saha, Auromeet and Niranjan, K., *ibid*, 2001, **80**, 145–150.
8. Ramanathan, V. *et al*., Indian Ocean Experiment, White Paper, C[4], Scripps Institution of Oceanography, La Jolla, CA 92093–0221, USA, 1995.
9. Niranjan, K. *et al*., *Tellus*, 1997, **49B**, 439–446.
10. Doerffer, R. GKSS 92/E/54, GKSS-Forschungszentrum Geesthacht GMBH, 1992.
11. Indian Remote Sensing Satellite IRS P4 (OCEANSAT) Handbook, National Remote Sensing Agency, Department of Space, Government of India, Hyderabad, 1999.
12. Gordon, H. R., *J. Geophys. Res.*, 1997, **102**, 17081–17106.
13. Okada, Y., Mukai, S. and Sano, I., *J. Indian Soc. Remote Sensing*, 2002 (in press).
14. Rajeev, K., Ramanathan, V. and Meywerk, J., *J. Geophys. Res.*, 2000, **105**, 2029–2043.
15. Angstrom, A., *Tellus*, 1961, **13**, 214–223.
16. Shaw, G. E., Regan, J. A. and Herman, B. M., *J. Appl. Meteorol.*, 1973, **12**, 374–380.
17. Satheesh, S. K., *Curr. Sci.*, 2002, **82**, 310–316.
18. Moorthy, K. Krishna, Nair, Prabha R. and Murthy, B. V. Krishna, *J. Appl. Meteorol.*, 1990, **30**, 844–852.
19. Moorthy, K. Krishna, Pillai, Preetha S., Saha, Auromeet and Niranjan, K., *Curr. Sci.*, 1999, **76**, 961–967.
20. Moorthy, K. Krishna, Satheesh, S. K. and Murthy, B. V. Krishna, *J. Atmos. Solar-Terr. Phys.*, 1998, **60**, 981–992.

ACKNOWLEDGEMENTS. The OCM data were available to R.P.S. through the ISRO-AO project. The work was supported by a grant under ISRO-GBP programme from the Indian Space Research Organization, Bangalore to R.P.S. We thank the anonymous reviewers for their comments and suggestions.

Received 9 April 2002; revised accepted 19 September 2002

New chemical shift signatures of bound calcium in EF-hand proteins

H. S. Atreya and K. V. R. Chary*

Department of Chemical Sciences, Tata Institute of Fundamental Research, Mumbai 400 005, India

We present two new chemical shift signatures for monitoring the state of bound calcium (Ca^{2+}) in NMR studies of EF-hand proteins. They have been observed in the form of large upfield chemical shifts (1–1.5 ppm) for (i) $H^{\beta 1}/H^{\beta 2}$ and (ii) $^{13}C^{\beta}$ resonances of a conserved Asp residue at the first position of 12 amino acid residue long Ca^{2+}-binding loops, going from Ca^{2+}-free (apo) to the Ca^{2+}-bound (holo) form of protein. In the apo form, both the $H^{\beta 1}/H^{\beta 2}$ and $^{13}C^{\beta}$ spins are found to resonate at their normal chemical shift values. Such upfield-shifted resonances of the Asp residue, in the holo-form, are shown to arise due to the ring current effect of a conserved Phe/Tyr residue at –4 position, preceding the same Ca^{2+}-binding loop. This is illustrated in the case of calmodulin and four other proteins, belonging to the family of EF-hand proteins.

EF-hand proteins belong to a growing family of calcium (Ca^{2+})-binding proteins, with more than 1000 distinct sequences known and catalogued into 66 different subfamilies[1]. These proteins, which function as signal transducers or modulators, have been a subject of great interest for structural biologists, resulting in the availability of three-dimensional (3D) structures for more than 100 of them as of today[2]. The most well-studied proteins in this family are calmodulin (CaM)[3], troponin C (TnC)[4], calbindin[5] and parvalbumin[6].

The canonical Ca^{2+}-binding motif in EF-hand proteins consists of a contiguous 12-residue loop flanked by two helices forming the so-called 'EF-hand motif'[7]. According to the convention, such Ca^{2+}-binding sequence is termed the EF-'loop' or the Ca^{2+}-binding loop, although the last three positions in it initiate the second helix (or the F-helix). Each of the flanking helices is amphiphilic and possesses four conserved hydrophobic residues at positions –1, –4, –5 and –8 in the first helix (E-helix), and positions 13, 16, 17 and 20 in the second helix (F-helix)[7]. The numbering is relative to the Ca^{2+}-binding loop. In such canonical Ca^{2+}-binding loop, the specific sites labelled as *X*, *Y*, *Z*, *–Y*, *–X*, *–Z* in Table 1, refer to 1st, 3rd, 5th, 7th, 9th and 12th positions respectively, in the Ca^{2+}-binding loops of the protein, which co-ordinate to Ca^{2+} in a pentagonal bi-pyramidal geometry[7]. Out of these, residues at positions 1, 3, 5 and 12 co-ordinate directly to Ca^{2+} via their side-chain carboxylate/carbonyl groups. Table 1 shows the primary sequence of Ca^{2+}-

*For correspondence. (e-mail: chary@mailhost.tifr.res.in)